catalysts

MDPI

Article

Selective Synthesis of 1,4-Dioxane from Oxirane Dimerization over ZrO_2/TiO_2 Catalyst at Low Temperature

Yinan Wang [1], Qingrong Yu [2], Lijun Xue [1], Qingyue Yu [1,*] and Xinbao Zhu [3,*]

[1] School of Chemical, Material and Environment Engineering, Nanjing Polytechnic Institute, Nanjing 210048, China; wangyinan@njpi.edu.cn (Y.W.); xuelijun@njpi.edu.cn (L.X.)
[2] Hailing Middle School of Haian, Nantong 226600, China; cnjsyqr@126.com
[3] School of Chemical Engineering, Nanjing Forestry University, Nanjing 210037, China
* Correspondence: qingyueyunj@126.com (Q.Y.); zhuxinbao@njfu.com.cn (X.Z.)

Abstract: We report a route to produce 1,4-dioxane from oxirane by using ZrO_2/TiO_2 as catalyst. The composite oxide ZrO_2/TiO_2 was prepared by a coprecipitation method and the catalytic performance was tested through the synthesis of 1,4-dioxane from oxirane in a pipe reactor. The X-ray diffraction (XRD) shows that ZrO_2 and TiO_2 are in crystal form. When the mass percentage of ZrO_2 is 25%, the composite oxide ZrO_2/TiO_2 presents as an amorphous form. The sample 25%ZrO_2/TiO_2 exhibits a specific surface area of 269.5 $m^2 \cdot g^{-1}$ and pore volume of 1.34 $mL \cdot g^{-1}$. The catalyst has 670 $\mu mol \cdot g^{-1}$ of NH_3-TPD acid, and the characterization of ammonia infrared spectroscopy (NH_3-FTIR) shows that both Brønsted and Lewis acids are present on the surface of the catalyst. The reaction mechanism was analyzed according to the distribution of product. The test of catalytic performance showed 100.0% conversion of oxirane and 86.2% selectivity of 1,4-dioxane at the optimal operation conditions: atmospheric pressure, reaction temperature 75 °C and gaseous hourly space velocity of 1200.0 h^{-1}. The catalyst exhibits good catalytic performance stability after continuous use for 720 h.

Keywords: 1,4-dioxane; oxirane; zirconium dioxide; titanium dioxide; reaction mechanism

Citation: Wang, Y.; Yu, Q.; Xue, L.; Yu, Q.; Zhu, X. Selective Synthesis of 1,4-Dioxane from Oxirane Dimerization over ZrO_2/TiO_2 Catalyst at Low Temperature. *Catalysts* **2022**, *12*, 832. https://doi.org/10.3390/catal12080832

Academic Editors: Zongjian Liu and Jun Li

Received: 28 June 2022
Accepted: 26 July 2022
Published: 29 July 2022

1. Introduction

1,4-Dioxane (DIOX), as an aprotic polar solvent with a fragrance, has many uses beyond its key role as a stabilizer for many chemicals [1,2]. It is used directly in several industrial and commercial processes and is found in a wide range of consumer products, such as in medicine, perfume, brightener, aseptic, synthetic leather as well as in special fine chemicals production, etc. [3–6]. 1,4-dioxane also occurs as a by-product in the production of certain surfactants, synthetic textiles, plastics, and resins [1]. 1,4-Dioxane can also be used in the new energy field. Ding et al. [7] found 1,4-dioxane could be used in passivating lithium electrodes. Choi et al. [8] reported that 1,4-dioxane diol derivative compound was applied as secondary battery electrolyte additive used in an electrolyte solution for a lithium secondary battery. Yamaji et al. [9] discovered 1,4-dioxane could replace lithium ion secondary battery electrolyte.

In industrial processes, there are many side reactions in the production of 1,4-dioxane from ethylene glycol dehydration with concentrated sulfuric acid and the purity of 1,4-dioxane is very low [1,10,11]. Moreover, corrosion by sulfuric acid leads to high requirements for manufacturing equipment. Serious environmental pollution should also be considered because of high volumes of wastewater and industrial salt from the neutralization of sodium hydroxide with sulfuric acid.

To develop a green and economic 1,4-dioxane synthesis process, much work has been performed by many researchers. Tian's team [12] synthesized 1,4-dioxane from ethylene glycol by reactive distillation. Wen's group [13] produced 1,4-dioxane from diethylene glycol over the catalyst p-toluene sulphonic acid. Some publishes patents also disclosed the technical details of 1,4-dioxane synthesis. Lee and partners [14,15] reported

the preparation of 1,4-dioxane from ethylene glycol-containing waste, and the process for the preparation of 1,4-dioxane from the bottom residue of oxidized ethylene/ethylene glycol plants, respectively. Hu and Yang [16] obtained 1,4-dioxane from reaction of ethanol and ethylene glycol in a solution mixture. Anil's group [17] found the process for preparation of 1,4-dioxane, involving diethylene glycol to catalytic dehydration in the presence of solid acid or super acid catalysts. Sivaev and coworkers [18] reported the practical synthesis of a 1,4-dioxane derivative of the closo-dodecaborate anion and its ring opening with acetylenic alkoxides.

Normally the synthesis of 1,4-dioxane is catalyzed by homogeneous catalysts. While the molecular sieve as a catalyst could overcome these shortcomings, such as the sulfuric acid catalytic process for synthesis. However, the molecular sieve catalyzed reaction takes place usually under a relatively high temperature, 160 °C [19,20]. The acid property is an important factor influencing the performance of a solid acid catalyst [21]. Aponte and Lasa [19] believed that catalyst selectivity was related to the amount of the acids with appropriate strength. Our group [22] found that the synergy of Brønsted and Lewis acids has significant effects to improve the conversion of raw material. The catalyst ZrO_2/TiO_2 possesses stronger surface acid properties, better heat stability and larger specific surface area [23], is widely used in catalytic cracking [24], performs cyclohexanone oxime Beckmann rearrangement [25], removes chlorofluorocarbons [26], performs hydrogenation desulfurization [27], electrochemical hydrogen evolution [28] and car exhaust catalytic removal oxynitride reactions [29], and other industrial catalyzed reactions. However, ZrO_2/TiO_2 has not been found in the catalytic synthesis of DIOX with oxirane (or ethylene oxide, EO) in the literature.

In this work we prepared the composite oxide ZrO_2/TiO_2 to synthesize 1,4-dioxane from ethylene oxide at low temperature. It is meaningful, due to the atomic economics of the reaction and there is no waste to pollute the environment. The catalyst does not cause corrosion of the equipment. The mechanism of the synergy of B acid and L acid is explored to increase efficiency of ethylene oxide conversion and 1,4-dioxane yield.

2. Results and Discussion

2.1. Morphological Analysis

Figure 1 displays the XRD patterns of TiO_2, ZrO_2 and composite oxide 25%ZrO_2/TiO_2 catalysts. The ZrO_2 sample exhibited the characteristic diffraction peaks of monoclinic crystal with 2θ = 28.3°, 31.2° and 50.3°. This result indicates that the zirconium hydroxide is reduced to zirconium dioxide monoclinic crystal during the calcination process. The characteristic diffraction peaks of TiO_2 at 25.4°, 48.1° and 54.7° are attributed to the anatase structure, so the titanium hydroxide decomposes to titanium dioxide in the calcination process. The composite oxide sample 25%ZrO_2/TiO_2 shows an amorphous form, while the characteristic diffraction peaks of ZrO_2 and TiO_2 have disappeared [30].

Dehydration of zirconium hydroxide generates zirconium oxide at high temperature, and titanium hydroxide dehydrates to form titanium oxide with calcination. Oxidation of polyethylene glycol removes the template agent from the flocculation samples at high temperature. These complex interactions occurr inside ZrO_2, TiO_2, and ZrO_2 with TiO_2, which produce ZrO_2 and TiO_2 crystal particles, and the amorphous aggregate ZrO_2/TiO_2 sample [30,31].

2.2. Properties and Activities of Catalysts

The acid properties of the samples were measured by NH_3-FTIR. It is generally believed that the absorption peaks at 1610 and 1230–1260 cm^{-1} are ascribed to the vibration of coordination adsorbed NH_3 on Lewis acid sites, and the absorption peaks at 1393, 1450, and 1680 cm^{-1} could be attributed to NH^{4+} adsorbed vibration on Brönsted acid sites [32–35]. As shown in Figure 3, the ZrO_2 sample has both L acid and B acid peak sites. The peak at 1430 cm^{-1} is attributed to the ammine ions adsorbed on B acid sites, and the peak at 1607 cm^{-1} and 1267 cm^{-1} are attributed to the ammine ions adsorbed on L acid sites,

respectively. The peak of the TiO_2 sample at 1601 cm^{-1} is attributed to the ammine ions absorbed on L acid sites. The composite oxide 25% ZrO_2/TiO_2 sample also has L acid and B acid peak sites. The peak of at 1437 cm^{-1} is attributed to the ammine ions adsorbed on B acid sites, and the peak at 1605 cm^{-1} and 1267 cm^{-1} are attributed to the ammine ions adsorbed on L acid sites, respectively. Compared with ZrO_2, the peak area of composite oxide 25%ZrO_2/TiO_2 sample at 1437 cm^{-1} transmission peak area is larger and the intensity is increased. Thus the B acid content of 25%ZrO_2/TiO_2 is enhanced significantly. Shen [36,37] reported the measurements of infrared spectra using the pyridine as the probe molecule; the result reported that only Lewis acid sites were detected. Besides pyridine as the probe molecule, the probe molecule of 2,6-dimethylpyridine which could detect Brönsted acid sites was also used to perform the measurement of infrared spectra [33]. The references results are in accordance with the results of this paper.

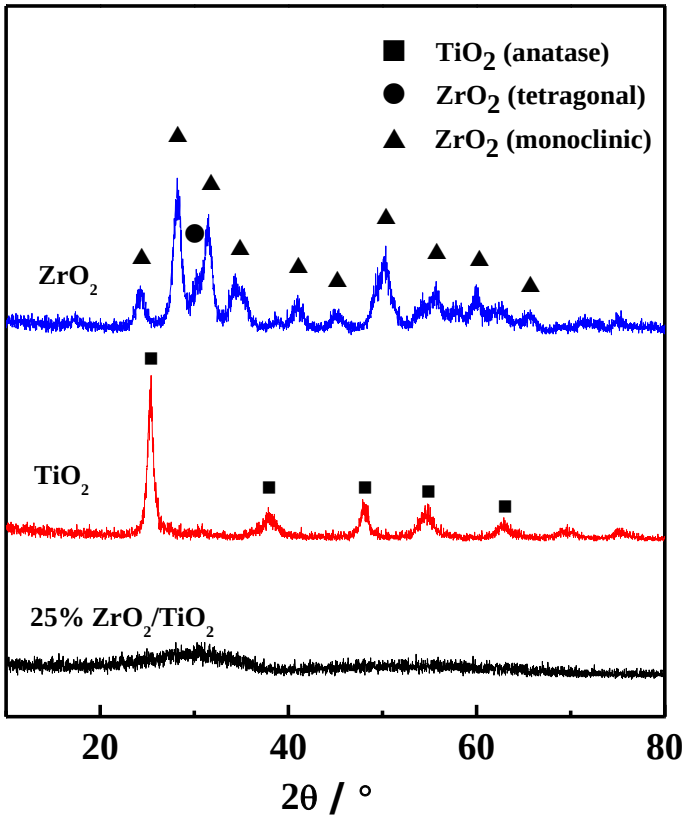

Figure 1. XRD patterns of samples.

The TEM images of TiO_2, ZrO_2 and 25%ZrO_2/TiO_2 samples are showed in Figure 2a–c. Both TiO_2 and ZrO_2 are mainly accumulated large grains with regular particle shape, and the composite oxide 25%ZrO_2/TiO_2 represents an aggregated form with high heap density particles, which are different from TiO_2 and ZrO_2.

Table 1 presents the specific surface area, pore volume and ammonia adsorption capacity of xZrO_2/TiO_2 catalysts. Due to the dehydration and oxidation of polyethylene glycol to remove the template agent at high temperature, there are complex interactions between ZrO_2 and TiO_2, which leads to more mesopores and micropores in the xZrO_2/TiO_2 sample. It can be seen that ZrO_2/TiO_2 has larger specific surface area, pore volume and NH_3 adsorption capacity, compared with ZrO_2 and TiO_2. The ratio of the Brönsted and Lewis acidic site's densities is according to the ratio of the corresponding characteristic peak area. The actual NH_3 adsorption amount of the Brönsted and Lewis acidic sites are allocated according to the characteristic peak area ratio from the total NH_3 adsorption. The sample TiO_2 has no Brönsted acidic site. And TiO_2 has no activity for the dimerization of EO into 1,4-dioxane, while the dimerization activity of ZrO_2 is low. As the content of

ZrO_2 is adjusted, the ratio of B acid to L acid of ZrO_2/TiO_2 is optimized, and the total acid content is increased, the EO ring-opening reaction activity of ZrO_2/TiO_2 is enhanced. When the ZrO_2 mass amount is 25% in ZrO_2/TiO_2, the catalyst possesses the maximum acid amount, the conversion of ethylene oxide over ZrO_2/TiO_2 catalyst is 100%, and the selectivity of DIOX is 86.2%.

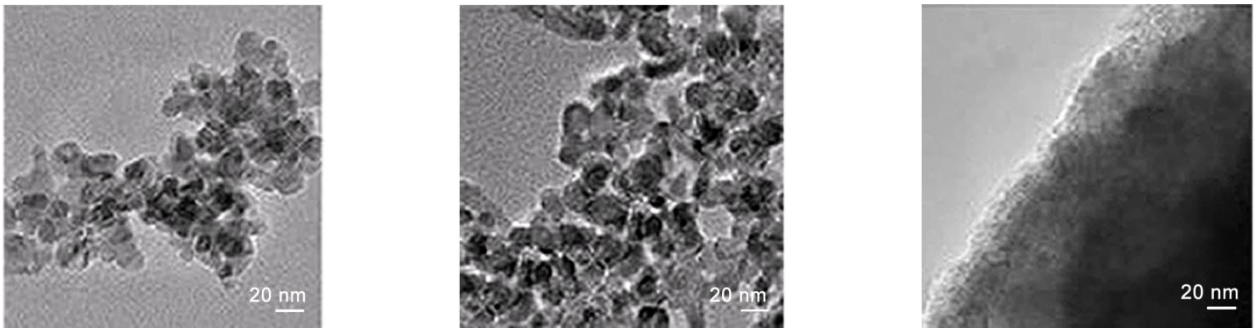

(**a**) TiO_2 (**b**) ZrO_2 (**c**) 25%ZrO_2/TiO_2

Figure 2. TEM images of samples.

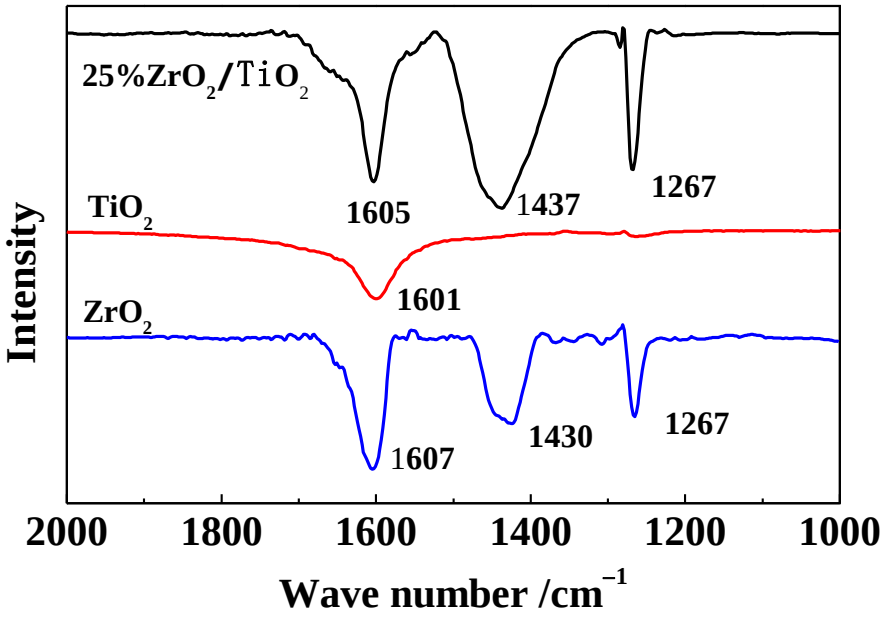

Figure 3. NH_3-FTIR spectrum of samples.

Table 1. Surface area, pore volume, NH_3 adsorption amount and catalytic performance of samples.

Sample	S_{BET}, $m^2 \cdot g^{-1}$	V_P, $mL \cdot g^{-1}$	NH_3 *ads*, $\mu mol \cdot g^{-1}$		*Con.* of EO, %	*Sel.* of DIOX, %
			L-acid	B-acid		
TiO_2	87.2	1.09	448	0	0	0
5%ZrO_2/TiO_2	120.7	1.21	303	132	63.1	41.8
15%ZrO_2/TiO_2	168.2	1.22	298	218	86.7	52.6
20%ZrO_2/TiO_2	189.1	1.46	279	322	99.2	61.3
25%ZrO_2/TiO_2	269.5	1.34	227	443	100.0	86.2
50%ZrO_2/TiO_2	210.3	1.26	213	344	100.0	66.4
75%ZrO_2/TiO_2	175.5	1.08	206	288	100.0	59.6
ZrO_2	90.1	1.17	182	179	100.0	41.5

Note: Reaction temperature 75 °C, GHSV 1200 h^{-1}, stable for 120 h.

2.3. Distribution of Product and Reaction Principle

According to the characterization of the products, ethylene oxide might be involved in the following reactions under the acid catalytic reaction:

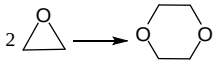
(1)

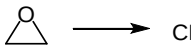
(2)

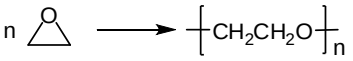
(3)

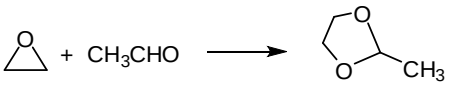
(4)

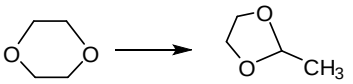
(5)

Dimerization of EO leads to the synthesis of DIOX, which is the main reaction (Equation (1)). EO is isomerized to form acetaldehyde by EO ring-opening reaction (Equation (2)); EO is also polymerized to form polyethylene glycol ether (Equation (3)); Acetaldehyde, the isomerization product of ethylene oxide, reacts with ethylene oxide to form 2-methyl-1,3-dioxy-pentane (DIOXOL) (Equation (4)); DIOX is isomerized to 2-methyl-1,3-dioxy-pentane over catalyst (Equation (5)).

2.4. Mechanism Analysis of Main Reaction

The trace moisture on the surface of the catalyst changes the amount ratio of B acid and L acid catalyst [1,30]. The synergy of B acid and L acid significantly increases the efficiency of ethylene oxide conversion and 1,4-dioxane yield. According to these phenomena of the process, the mechanism for 1,4-dioxane synthesis from ethylene oxide over ZrO_2/TiO_2 catalyst is shown in Figure 4.

Trace water is adsorbed on the surface of catalyst ZrO_2/TiO_2 (Path 1) and is decomposed to form the B acid site (Path 2) at the surface active center. EO diffuses and interacts with the B acid (Path 3), and the ring of EO is opened to form a carbocation at the B acid site (Path 4). EO spreads to the surface of ZrO_2/TiO_2 (Path 5) and is chemically adsorbed at the L acid center on the surface of the catalyst (Path 6). With the polarization of L acid, the electron transfer occurs in EO. When the C–O bond of EO breaks and the ring opens (Path 7), then the ring-opened EO at the L acid center combines with the ring-opened carbocation of EO at the B acid site to form an intermediate state (Path 8). A water molecule leaves from the intermediate and recycles back to the surface of the catalyst (B acid regenerates from the intermediate state) (Path 9). DIOX is formed after the B acid and L acid are regenerated (Path 10). The product DIOX is released from the high concentration surface of the catalyst (Path 11).

2.5. Effects of Space Velocity and Temperature

Under atmospheric pressure, a temperature of 75 °C, the effect of gaseous hourly space velocity on the isomerization of EO to DIOX over catalyst 25%ZrO_2/TiO_2 is shown in Table 2.

At higher space velocity, contact time will be shorter for the interaction between EO and the catalyst surface active center, which leads to lower conversion of EO and more production of the acetaldehyde isomer. When GHSV is 1800 h^{-1}, the conversion of ethylene oxide is 63.9%. Long residence time at low space velocity results in acetaldehyde continuing to react with EO to generate DIOXOL. The isomerization of DIOX also produces more

DIOXOL. The polymerization of acetaldehyde manufactures polyacetaldehyde. When GHSV is 600 h^{-1}, the conversion of EO reaches 100.0%.

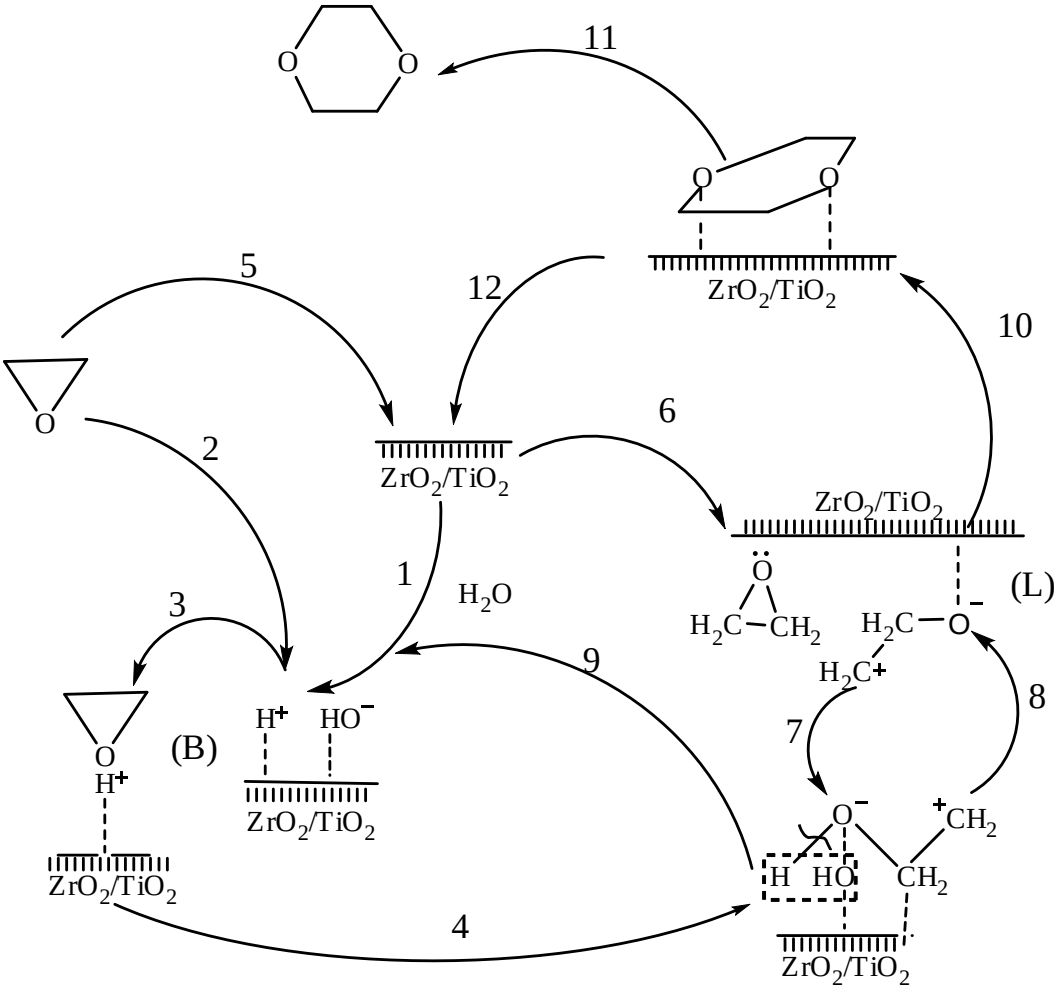

Figure 4. Diagram of synthesis of 1,4-dioxane from ethylene oxide.

Table 2. Effect of GHSV.

GHSV, h^{-1}	Con. of EO, %	Distribution of Products, %			
		AC	DIOXOL	DIOX	Others
600	100.0	4.7	16.2	64.7	14.4
1200	100.0	5.2	4.7	86.2	3.9
1800	63.9	15.3	3.9	63.0	17.8

Notes: AC: acetaldehyde; DIOXOL: 2-methyl-1,3-dioxolame; DIOX: 1,4-dioxane; Others: -$[CH_2CH_2O]_n$- and metacetaldehyde.

The effect of reaction temperature on the dimerization of EO is shown in Table 3.

Table 3. Effect of reaction temperature.

Reaction Temp., °C	Con. of EO, %	Distribution of Products, %			
		AC	DIOXOL	DIOX	Others
65	86.7	32.6	8.4	53.8	5.2
75	100.0	5.2	4.7	86.2	3.9
85	100.0	3.6	22.2	58.2	16.0

Notes: AC: acetaldehyde; DIOXOL: 2-methyl-1,3-dioxolame; DIOX: 1,4-dioxane; Others: -$[CH_2CH_2O]_n$- and/or metacetaldehyde.

At 65 °C, the conversion of EO is 86.7%, and the isomerization product acetaldehyde is 32.6%. At 75 °C, the conversion of EO is 100.0%, and the proportion of acetaldehyde is decreased to 5.2%. When the temperature is 85 °C, the proportion of acetaldehyde, is decreased to 3.6%, while the corresponding contents of 2-methyl-1,3-dioxane and 1,4-Dioxane are increased significantly. When the temperature is low, the speed of the EO ring-opening reaction is slow, which leads to the high proportion of isomerism of EO. With the increase in temperature, the conversion of EO becomes higher but more 2-methyl-1,3-dioxy-pentane is produced.

2.6. Stability of Catalyst

The effect of reaction time on the conversion of EO and the selectivity of DIOX over 25%ZrO_2/TiO_2 under atmospheric pressure, temperature 75 °C, and GHSV 1200 h^{-1} are shown in Table 4. In the initial reaction stage, EO is completely transformed, the main reaction and side reactions are active, and the DIOX selectivity reaches 61.3%. With the prolonging of reaction time, the surface-active center of the catalyst tends to be homogenous, leading to the selectivity of DIOX gradually stabilizing and reaching 82.6%. The catalyst activity maintains 100% conversion of EO when reaction time is 120 h. After 720 h, the activity and selectivity of the catalyst did not change significantly.

Table 4. Effect of reaction time.

Reaction Time, h	Con. of EO, %	Selectivity of DIOX, %
10	100.0	61.3
60	100.0	72.8
120	100.0	82.6
720	99.6	87.2

Reaction conditions: 25% ZrO_2-/TiO_2, atmospheric pressure, 75 °C, GHSV: 1200 h^{-1}.

With increasing duration, the surface-active center of TiO_2/ZrO_2 tends to be homogenous, leading to the selectivity of 1,4-dioxane stabilizing. Long time periods of oxirane dimerization can produce large molecular weight products, such as polyethylene glycol ether, which covers the catalyst active surface, and leads to conversion decreases. At the same time, the trace harmful impurities in oxirane can poison the catalyst. This is another reason why the conversion decreases slightly.

3. Materials and Methods

3.1. Materials

Ethylene oxide (99.0%), ammonia (98.0%), high purity nitrogen (99.99%) were provided by Nanjing Special Gas Plant (Nanjing, China) in AR-grade. Ethanol (99.9%, AR) was provided by Nanjing Chemical Reagent Co., Ltd. (Nanjing, China). Titanium tetrachloride (CR) was provided by Shanghai Sinopharm Group Chemical Reagent Co., Ltd. (Shanghai, China). Zirconium oxychloride (AC) was provided by Shanghai Lingfeng Chemical Reagent Co., Ltd. (Shanghai, China).

3.2. Preparation

The xZrO_2/TiO_2 catalysts were prepared according to our previous work [22] with necessary modifications. 0.10 mol·L^{-1} titanium tetrachloride in ethanol solution, 0.05 mol·L^{-1} zirconium oxychloride in aqueous solution, and the mass fraction of 5.0% polyethylene glycol of the aqueous solution were prepared, respectively. The polyethylene glycol aqueous solution was strongly stirred while dropping ammonia to adjust pH value of the solution in the range of 8.0 to 9.0. At the same time, zirconium oxychloride aqueous solution and titanium tetrachloride ethanol solution were added, respectively. The component content of the composite oxide is accomplished by controlling the drip amount of zirconium oxychloride solution and titanium tetrachloride ethanol solution, denoted as xZrO_2/TiO_2 (x is the mass fraction of ZrO_2). The flocculent precipitates were filtered and washed to neutral,

then dried at room temperature for 24 h, followed by drying at 120 °C for 12 h, and calcined at 550 °C for 6 h to get the ZrO_2/TiO_2 composite oxide.

3.3. Characterization

XRD patterns were analyzed by D8 ADVANCE of Bruker (German) with CuKa radiation (λ = 0.15406 nm) operated at 40 kV and 40 mA. The 2θ angle was scanned in the range of 10~80°. The BET surface area of catalysts were detected by N_2 adsorption with an adsorption analyzer (Omnisorp-100CX volumetric). Prior to N_2 adsorption measurements, the sample was evacuated at 200 °C for 12 h. And the specific surface area was calculated by the BET method. The average pore diameters and pore volumes were calculated by the BJH method with the desorption branches of the isotherms.

The IFS66V FTIR spectrophotometer of Brucker (Saarbruechen, German) was used to measure the ammonia adsorption infrared spectra. The self-supporting wafer with a diameter of 13 mm was pressed by the sample of 15 mg, and was then set in an IR cell connecting with a vacuum system. After the proper treatment of the wafer, the spectrum was recorded as a background. Then the spectrum was recorded when 3 kPa of NH_3 was introduced into the IR cell, and the adsorption process was performed for 10 min. Finally, the system was evacuated for 15 min. A spectrum of adsorbed species was obtained by subtracting the background spectrum of the wafer. The recorded spectrum was obtained by 40 scans, and the resolution was 4 cm^{-1}.

3.4. Reaction

All tests for 1,4-dioxane and possible intermediates and by products were carried out in a stainless pipe reactor (PR-60-DRL, Nanjing Anding Chemical Science & Technology Co., Ltd, Nanjing, China) and the detailed procedure is described as follows. 5.0 g catalyst mixed with silica sand was added into the pipe in the flat-temperature zone of the reactor. The reactor was sealed and flushed with pure N_2 to remove the air residue. Liquid ethylene oxide was added from the cylinder into the vaporizer. The vaporized ethylene oxide kept at 50 °C was measured by mass flowmeter and mixed with high purity nitrogen at the preheater. Then the mixed gases were guided into the entrance of the reactor. Finally, the pipe reactor was filled with ethylene oxide and nitrogen mixed gases to a desired pressure 0.1~1 MPa. The reactor was heated to several temperature points (55, 65, 75, 85, 95 °C) with different pressure (0, 0.1, 0.2, 0.3, 0.4 MPa). The mixture products were collected in liquid-vapor separator cooling by 12 °C ethanol refrigerant. The tail gas was cooled down by ethanol refrigerant of 0 °C to collect unreacted ethylene oxide, while the nitrogen was exhausted to the air. Using a sampling bag, the gas was collected for further analysis to avoid polluting the environment.

3.5. Analysis

GC-MS (Thermo Finnigan, Waltham, MA, USA, quartz capillary column, 30 m × 0.32 mm × 0.5 μm) with a FID detector was used to confirm the products. The temperature of the column is 40 °C and that of the detector is 260 °C. The collected products and tail gas were analyzed by GC (Lu'nan, Linyi, China, FFAP capillary column), equipped with TCD and FID detectors.

The oxirane conversion was calculated by Equation (1):

$$Conversion = \frac{B_{oxirane} - A_{products}}{B_{oxirane}} \times 100\% \quad (6)$$

The products selectivity's were calculated by Equation (2):

$$Selectivity = \frac{n_i k_i M_{(C_2H_4O)}}{2(B_{oxirane} - B^*_{oxirane})} \quad (7)$$

where $B_{oxirane}$ $B^{*}_{oxirane}$ and $A_{products}$ represent the oxirane weight before and after reaction, and the products weight, respectively. n_i presents the mole number of product i; k_i represents the number of carbon atoms in product i; $M_{(C_2H_4O)}$ represents the molecular weight of the oxirane unit.

4. Conclusions

The composite oxide ZrO_2/TiO_2 was prepared by a coprecipitation method. ZrO_2 and TiO_2 were in the crystal, as shown by X-ray diffraction. When the mass percentage of ZrO_2 was 25%, the 25%ZrO_2/TiO_2 presents as an amorphous form, and the specific surface area is 269.5 $m^2 \cdot g^{-1}$ and pore volume is 1.34 $mL \cdot g^{-1}$. This sample has 670 $\mu mol \cdot g^{-1}$ of NH_3-TPD acid amount, and the ammonia infrared spectroscopy showed that both Brønsted and Lewis acids are presented on the catalyst surface. The surface B acid could be converted from trace water. And B acid and L acid synergistically catalyze ethylene oxide to produce 1,4-dioxane.

Reaction mechanism was analyzed according to the distribution of product. The test of catalytic performance showed 100.0% conversion of oxirane and 86.2% selectivity of 1,4-dioxane at the optimal operation conditions: atmospheric pressure, reaction temperature 75 °C and gaseous hourly space velocity of 1200.0 h^{-1}.

After 720 h, the conversion of ethylene oxide is 99.6% and the selectivity of 1,4-dioxane is 87.2%. The catalyst showed high activity and good stability for selective synthesis of 1,4-dioxane from oxirane at low temperature.

Author Contributions: Y.W., Q.Y. (Qingyue Yu) and X.Z. conceived and designed the experiments; Y.W., Q.Y. (Qingrong Yu) and L.X. performed the experiments; Y.W. and L.X. analyzed the data and contributed the materials; Q.Y. (Qingyue Yu) contributed analysis tools; Y.W. and Q.Y. (Qingrong Yu) wrote the paper. All authors have read and agreed to the published version of the manuscript.

Funding: We are grateful to the following government agencies for their financial support: Chinese Jiangsu Co-Innovation Center of Efficient Processing and Utilization of Forest Resources, and Chinese Jiangsu Province Key Research and Development Program (BE-2019111).

Acknowledgments: We thank Jun Li from the State Key Laboratory of Materials-Oriented Chemical Engineering of Nanjing Tech University for the discussion on reaction mechanism and the linguistic modification.

Conflicts of Interest: The authors declare no conflict of interest.

References

1. Mohr, T.K.G. 1,4-Dioxane Chemistry, Uses, and Occurrence. In *Environmental Investigation and Remediation: 1,4-Dioxane and Other Solvent Stabilizers*; Stickney, J.A., Diguiseppi, W.H., Eds.; CRC Press: Boca Raton, FL, USA, 2010; pp. 75–114.
2. Kazachenko, A.S.; Akman, F.; Malyar, Y.N.; Issaoui, N.; Vasilieva, N.Y.; Karacharov, A.A. Synthesis optimization, DFT and physicochemical study of chitosan sulfates. *J. Mol. Struct.* **2021**, *1245*, 131083. [CrossRef]
3. Xie, W.Z.; Liu, H.; Tang, X.; Zeng, X.H.; Sun, Y.; Ke, X.X.; Li, T.Y.; Fang, H.Y.; Lin, L. Efficient synthesis of 2,5-furandicarboxylic acid from biomass-derived 5-hydroxymethylfurfural in 1,4-dioxane/H_2O mixture. *Appl. Catal. A Gen.* **2022**, *630*, 118463. [CrossRef]
4. Rana, M.M.; Rajeev, A.; Natale, G.; Siegler, H. Effects of synthesis-solvent polarity on the physicochemical and rheological properties of poly(N-isopropylacrylamide) hydrogels. *J. Mater. Res. Technol.* **2021**, *13*, 769–786. [CrossRef]
5. Aramita, D.; Sougata, S.; Khalymbadzha, A.I.; Zyryanov, V.G.; Majee, A. A practicable synthesis of 2,3-disubstituted 1,4-dioxanes bearing a carbonyl functionality from α,β-unsaturated ketones using the Williamson strategy. *Org. Biomol. Chem.* **2021**, *19*, 1278–1286.
6. Gabrielle, R.S.; Jacob, G.; Denis, G. Annulative dimerization of carbohydrates: Synthesis of complex C2-Symmetrical 1,4-dioxane-sugar hybrids. *Eur. J. Org. Chem.* **2021**, *22*, 3322–3330.
7. Ding, F.; Zhang, C.F.; Hu, X.G. Passivating lithium electrodes with 1,4-dioxane. *Rare Met. Mater. Eng.* **2006**, *35*, 585–588.
8. Choi, H.Y.; Lee, J.; Kang, J.; Lee, D.K.; Jung, P.; Cho, C.; Cho, S. Secondary Battery Electrolyte Additive Used in Electrolyte Solution for Lithium Secondary Battery, Comprises 1,4-Dioxane Diol Derivative Compound. Korea Patent KR2022023139A, 2 March 2022.
9. Yamaji, T.; Sugiyama, Y.; Iwata, H.; Watanabe, Y.; Sugioka, T. Electrolyte Solution for Secondary Battery e.g., Lithium Ion Secondary Battery Contains Electrolyte, the Tetrahydropyran Which May Be Substituted by the Alkyl Group, and 1,4-Dioxane. Japan Patent JP2020177814, 29 October 2020.

10. Liu, J.f. Synthesis of 1,4-dioxane from the mixture of diethylene glycol and ethane diol over hetreropolyacid. *Chin. Ind. Catal.* **2000**, *8*, 28–30.
11. Heuvelsland, J.A. Method for Producing 1,4-Dioxane. U.S. Patent US4764626, 16 August 1988.
12. Li, S.; Wang, T.; Tian, H. Synthesis of 1,4-dioxane from ethylene glycol by reactive distillation. *Nat. Gas Chem. Ind.* **2017**, *42*, 69–72,107.
13. Wen, R.; Luo, X.; Yu, S. Catalytic synthesis of 1,4-dioxane from diethylene glycol using p-toluene sulphonic acid as a catalyst. *Chin. J. Synth. Chem.* **2002**, *10*, 71–72.
14. Lee, K.; Lee, Y.; Jang, H. Preparation of 1,4-Dioxane from Ethylene Glycol-Containing Waste. KR1019930017899B1, 1 January 1997.
15. Lee, K.; Lee, Y. Process for the Preparation of 1,4-Dioxane from the Bottom Residue of Oxidized Ethylene/Ethylene Glycol Plant. KR100245197B1, 2 March 2001.
16. Hu, S.; Yang, W. Recovering Ethanol and Co-Producing Ethylene Glycol, Comprises e.g., Reacting Mixed Solution of Water, Ethanol and 1,4-dioxane with Ethylene Oxide, and Separating Obtained Crude Ethanol Containing Ethanol and 1,4-Dioxane. China Patent CN110835285A, 25 February 2020.
17. Anil, W.; Sheo, S.; Sreedharan, U.U.; Subramaniapillai, M. Process for Preparation of 1,4-Dioxane, Involves Subjecting Diethylene Glycol to Catalytic Dehydration in Presence of Solid Acid or Super Acid Catalysts. India Patent IN189099B, 14 December 2009.
18. Sivaev, I.B.; Kulikova, N.Y.; Bregadze, V.I. Practical synthesis of 1,4-dioxane derivative of the closo-dodecaborate anion and its ring opening with acetylenic alkoxides. *J. Organomet. Chem.* **2008**, *693*, 519–525. [CrossRef]
19. Aponte, Y.; Lasa, H. The effect of Zn on offretite zeolite properties: Acidic characterizations and NH_3-TPD desorption models. *Ind. Eng. Chem. Res.* **2017**, *56*, 1948–1960. [CrossRef]
20. Kiso, Y.; Tatsuo, O.; Yuki, K.; Kazuya, M.; Yuki, T.; Toshiro, Y. Molecular sieving effects of disk-shaped molecules on reverse osmosis and nanofiltration separation. *Sep. Purif. Technol.* **2017**, *173*, 286–294. [CrossRef]
21. Aliki, D.; Stamatina, V.; Papaspyridi, L.M.; Papaspyrides, C.D. A review on enzymatic polymerization to produce polycondensation polymers: The case of aliphatic polyesters, polyamides and polyesteramides. *Prog. Polym. Sci.* **2018**, *79*, 1–25.
22. Yu, Q.; Wang, J.; Yu, H. Preparation of ZrO_2-TiO_2 composite catalyst and its function for synthesis of tributyl citrate. *Chin. J. Process. Eng.* **2016**, *16*, 86–90.
23. Emad, N.; Al-Shafei, D.; Robert, B.; Katikaneni, S.P.; Hassan, A.; Al-Badairy, H.H. Direct conversion of CO_2 with methane into chemicals over ZrO_2/TiO_2 catalysts. *Chem. Eng. J.* **2021**, *491*, 129416.
24. Hisaki, K.; Kumiko, T.; Yuta, N.; Teruoki, T.; Takao, M. Catalytic cracking of heavy oil over TiO_2–ZrO_2 catalysts under superheated steam conditions. *Fuel* **2016**, *167*, 288–294.
25. Mehran, G.; Aghaei, H.; Abbaspur, A. Size-controlled synthesis of ZrO_2–TiO_2 nanoparticles prepared via reverse micelle method: Investigation of particle size effect on the catalytic performance in vapor phase Beckmann rearrangement. *Mater. Res. Bull.* **2008**, *43*, 1255–1262.
26. Lai, S.Y.; Pan, W.X.; Ching, F.N. Catalytic hydrolysis of dichlorodifluoromethane (CFC-12) on unpromoted and sulfate promoted TiO_2–ZrO_2 mixed oxide catalysts. *Appl. Catal. B Environ.* **2000**, *24*, 207–217. [CrossRef]
27. Kaluza, L. Activity of transition metal sulfides supported on Al_2O_3, TiO_2 and ZrO_2 in the parallel hydrodesulfurization of 1-benzothiophene and hydrogenation of 1-methyl-cyclohex1ene. *React. Kinet. Mech. Catal.* **2015**, *114*, 781–794. [CrossRef]
28. Singh, P.K.; Shin, C.H.; Lee, H.Y.; Razmjooei, F.; Sinhamahapatra, A.; Kang, J.; Yu, J.S. TiO_2/ZrO_2 Nanoparticle composites for electrochemical hydrogen evolution. *ACS Appl. Nano. Mater.* **2020**, *3*, 3634–3645. [CrossRef]
29. Masashi, K.; Kiyoshi, Y.; Hirofumi, S. Characterization and catalytic activity of CuO/TiO_2-ZrO_2 for low temperature CO oxidation. *Appl. Catal. A Gen.* **2017**, *547*, 199–204.
30. Wan, J.M.; Fu, L.; Yang, H.X.; Wang, K.; Xi, F.C.; Pan, L.S.; Li, Y.F.; Liu, Y.J. TiO_2-ZrO_2 composite oxide as an acid−base bifunctional catalyst for self-condensation of cyclopentanone. *Ind. Eng. Chem. Res.* **2020**, *59*, 19918–19928. [CrossRef]
31. Troitzsch, U.; Ellis, J.D. The ZrO_2-TiO_2 phase diagram. *J. Mater. Sci.* **2005**, *40*, 4571–4577. [CrossRef]
32. Tajima, M.; Niwa, M.; Fujii, Y.; Koinuma, Y.; Aizawa, R.; Kushiyama, S.; Kobayashi, S.; Mizuno, K.; Ohuchi, H. Decomposition of chlorofluorocarbons on W/TiO_2-ZrO_2. *Appl. Catal. B Environ.* **1997**, *14*, 97–103. [CrossRef]
33. Lahousse, C.; Aboulayt, A.; Maugé, F.; Bachelier, J.; Lavalley, J.C. Acidic and basic properties of zirconia-alumina and zirconia-titania mixed oxides. *J. Mol. Catal.* **1993**, *84*, 283–297. [CrossRef]
34. Manríquez, M.E.; López, T.; Gómez, R.; Navarrete, J. Preparation of TiO_2-ZrO_2 mixed oxides with controlled acid–basic properties. *J. Mol. Catal. A Chem.* **2004**, *220*, 229–237. [CrossRef]
35. Han, C.; Liu, B.; Zhang, H.; Shen, J. Characterization of TiO_2–ZrO_2 and isopropanol catalytic conversion. *Acta Phys.-Chim. Sin.* **2006**, *22*, 993–998. [CrossRef]
36. Shen, J.Y.; Cortright, R.D.; Chen, Y.; Dumesic, J.A. Microcalorimetric and infrared spectroscopic studies of γ–Al_2O_3 modified by basic metal oxides. *J. Phys. Chem.* **1994**, *98*, 8067–8073. [CrossRef]
37. Shen, J.Y.; Kobe, J.M.; Chen, Y.; Dumesic, J.A. Synthesis and surface acid/base properties of Magnesium-Aluminum mixed oxides obtained from hydrotalcites. *Langmuir* **1994**, *10*, 3902–3908. [CrossRef]